

Approaching transform-limited photons from nanowire quantum dots using excitation above the band gap

Patrick Laferrière,^{1,2,*} Aria Yin,^{1,2} Edith Yeung,^{1,2} Leila Kusmic,^{1,2} Marek Korkusinski,¹ Payman Rasekh,¹ David B. Northeast,¹ Sofiane Haffouz,¹ Jean Lapointe,¹ Philip J. Poole,¹ Robin L. Williams,¹ and Dan Dalacu^{1,2}

¹National Research Council Canada, Ottawa, Ontario, Canada K1A 0R6

²Department of Physics, University of Ottawa, Ottawa, Ontario, Canada K1N 6N5



(Received 12 August 2022; revised 24 March 2023; accepted 6 April 2023; published 19 April 2023)

We demonstrate that, even when employing above band gap excitation, photons emitted from semiconductor quantum dots can have linewidths that approach their transform-limited values. This is accomplished by using quantum dots embedded within bottom-up photonic nanowires, an approach which mitigates several potential mechanisms that can result in linewidth broadening: (i) Only a single quantum dot is present in each device, (ii) dot nucleation proceeds without the formation of a wetting layer, and (iii) the sidewalls of the photonic nanowire are comprised not of etched facets, but of epitaxially grown crystal planes. Using these structures we achieve linewidths of $2\times$ the transform limit for above band gap excitation. We also demonstrate a highly nonlinear dependence of the linewidth on both excitation power and temperature which can be described by an independent boson model that considers both deformation and piezoelectric exciton-phonon coupling. We find that for sufficiently low excitation powers and temperatures, the observed excess broadening is not dominated by phonon dephasing, a surprising result considering the high phonon occupation that occurs with above band gap excitation.

DOI: [10.1103/PhysRevB.107.155422](https://doi.org/10.1103/PhysRevB.107.155422)

I. INTRODUCTION

Quantum interference between two or more indistinguishable photons lies at the heart of most photonic quantum technologies [1] and high visibilities require highly coherent photons. Solid-state two-level emitters [2], e.g., epitaxial semiconductor quantum dots [3], can provide single photons with high efficiency provided they are incorporated within appropriate photonic structures supporting a single optical mode into which all photons are emitted. Within this solid-state environment, however, fluctuations in charge and spin or interactions with phonons can lead to broadening of the emitted photon linewidth compared to the Fourier transform limit and, consequently, a reduction of the two-photon interference visibility ν_{TPI} [4].

Excess broadening can be limited through the use of optical cavities [5,6] and resonant excitation [7], resulting in the observation of $\nu_{\text{TPI}} > 90\%$ between sequential photons emitted from the same source over timescales $> 1 \mu\text{s}$ [8,9]. Linewidths measured over longer timescales are, however, broadened compared to the transform limit [8,10], a broadening typically attributed to a slowly varying charge environment. One can therefore expect a reduction of ν_{TPI} for timescales longer than a few microseconds and, in the case of remote emitters [11–17] for which noise correlations are absent, the reduction may be particularly severe.

It is therefore essential to address the persistent broadening that arises from a time-dependent occupation of traps close

to the dot, producing a wandering of the exciton energy via the Stark effect [18]. These traps can be defects or impurities located in the bulk semiconductor material [19], at surfaces (e.g., the growth surface [20] or the etched sidewall surface [21]) or at epitaxial interfaces [22]. Additionally, quantum dots themselves are, by design, carrier traps and the impact on the linewidth, at least of crystal phase dots [23] (i.e., stacking faults), is well established [24].

In this paper we investigate a quantum dot system [25] distinct from the more conventional GaAs-based self-assembled dots [26] in several aspects that impact excess broadening. The dots are segments of InAsP within [0001] wurtzite-phase InP nanowires and are fabricated using a bottom-up technique. Here, the only surfaces in close proximity to the dot are the crystal lattice growth facets that make up the sidewalls of the nanowire, surfaces which have a lower defect density compared to the dry-etched sidewalls present in top-down structures [27]. Using the InP material system, we can also expect an order of magnitude reduction in the surface recombination velocity compared to GaAs [28]. The quantum dots are nucleated via a vapor-liquid-solid (VLS) growth process [29] in which no two-dimensional (2D) wetting layer forms, a layer associated with several broadening mechanisms in other dots [30]. The VLS growth mode is also unique in that the number of dots in each device is controlled [31] and by using devices that contain only a single emitter, potential charge fluctuations associated with carriers trapped in nearby quantum dots are eliminated.

We observe a significant reduction of excess broadening compared to conventional quantum dot emitters operated under the same conditions, with measured linewidths as low

*plaferr3@uottawa.ca

as $2\times$ the transform limit. Remarkably, these narrow lines are observed using above band gap excitation, i.e., conditions expected to promote fluctuations in the charge environment. We also find that, at sufficiently low temperatures, broadening due to phonon dephasing is insignificant with an onset for strong broadening observed for $T > 8$ K. This is similar to that observed using resonant excitation [30] and four-wave mixing techniques [32] and consistent with a significant reduction in ν_{TP1} observed in Ref. [33]. This behavior can be fully described by an independent boson model [34] that considers phonons propagating along the nanowire growth direction and which takes into account both deformation and piezoelectric exciton-phonon coupling. Importantly, to explain the nonlinearity we do not need to invoke virtual transitions between ground and excited states [33,35], for which the energy scales are inconsistent with our dot level structure. Instead, the nonlinearity is traced to the interplay of deformation and piezoelectric coupling mechanisms and their distinct dependence on phonon energy.

II. EXPERIMENTS

The nanowire-based devices were grown using chemical beam epitaxy on patterned substrates consisting of 20-nm gold catalysts centered in circular openings of a SiO_2 mask on an InP substrate using a two-step growth process [36]. First, a 20-nm-diameter InP nanowire core is grown using growth conditions that promote axial growth (e.g., low group V flux) and in this core we incorporate a ~ 5 -nm-thick $\text{InAs}_{0.25}\text{P}_{0.25}$ quantum dot. Second, the core is clad with a shell using growth conditions that promote radial growth (high group V flux). The resulting photonic nanowire has a base diameter of 250 nm that tapers to ~ 100 nm over a length of ~ 15 μm [Fig. 1(a)]. Photoluminescence (PL) spectra typically show emission from both the neutral exciton X and the negatively charged exciton X^{1-} at wavelengths of $\lambda \sim 970$ nm [see the inset in Fig. 1(b)].

Previously, we have used growth temperatures of 420°C for both the core and shell growths, which produced quantum dots emitting exciton photons with linewidths of 880 MHz, of which the inhomogeneous contribution was 730 MHz [37] and was associated with a high defect density in the InP causing charge fluctuations discussed above. In order to improve the material quality, in this study we increase the nanowire core growth temperature to 435°C . This temperature was thought to be an upper limit above which reasonable axial growth rates could not be maintained [38] and is discussed further below. For the shell growth we can access higher temperatures and here we study samples where the shell is grown at temperatures of $T_s = 450^\circ\text{C}$ to $T_s = 495^\circ\text{C}$.

Photoluminescence (PL) measurements were performed in a closed-cycle helium cryostat. The nanowire quantum dots were excited through a $100\times$ objective (numerical aperture of 0.81) and the emission was collected through the same objective and directed to a grating spectrometer equipped with a liquid nitrogen cooled charged-coupled device (CCD). For time-integrated PL measurements, the excitation was a continuous-wave laser operating at 780 nm, while for time-resolved measurements a pulsed laser operating at 670 nm was used. To measure linewidths, the dot emission was coupled

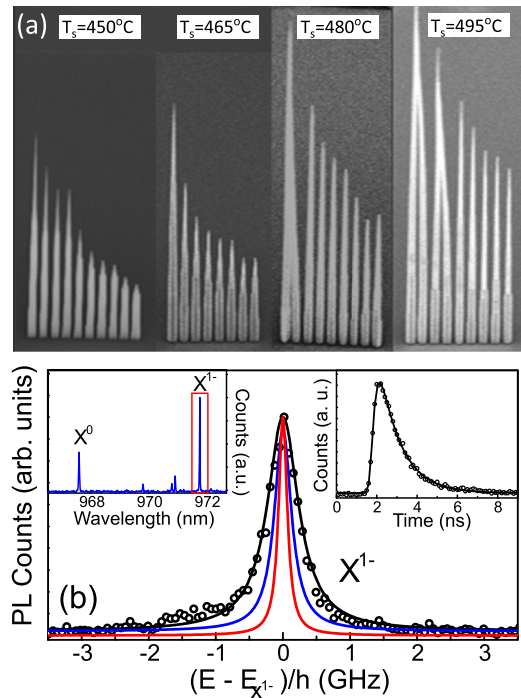


FIG. 1. (a) Scanning electron microscope images of linear arrays of nanowires pitched at 400 nm, each nanowire in an array having a different core diameter and each array grown at a different T_s ; see Ref. [36] for details. (b) High-resolution PL spectrum measured at 4 K and $P = 0.1P_{\text{sat}}$ (black open circles) of the X^{1-} line emission highlighted in the left inset. Also plotted are a Lorentzian fit to the data (black curve), the spectrum after deconvolution with the etalon response (blue curve), and the predicted transform-limited spectrum (solid red curve) calculated using the transition lifetime T_1 extracted from the PL decay curve shown in the right inset.

to a single-mode fiber and a single peak was selected using a fiber-based tunable filter with a 0.1 nm bandwidth. The spectral width of the filtered peak was resolved using a fiber-based, piezo-driven, scanning Fabry-Pérot etalon (bandwidth of 250 MHz, free-spectral range of 40 GHz) and detected with an avalanche photodiode.

We first look at the linewidth of an excitonic photon at low temperature (4 K) and low excitation power ($P = 0.1P_{\text{sat}}$) in a device where the shell is deposited at $T_s = 450^\circ\text{C}$. Figure 1(b) shows the high-resolution PL spectrum of an X^{1-} photon emitting at $E_{X^{1-}} = 1.276$ eV. The emission peak was fit with a Lorentzian function to extract the homogeneous linewidth which, after deconvolution with the etalon response, is $\delta_\omega = 322$ MHz. We note that fitting with a Voigt profile produced a negligible Gaussian contribution (i.e., we did not observe any significant inhomogeneous broadening). Using the radiative recombination lifetime of $T_1 = 1.02$ ns from the PL decay curve (see the inset in Fig. 1), we calculate the width of the transform-limited spectrum from $\delta_\omega = 1/2\pi T_1$. From these two widths we obtain the ratio $2T_1/T_2 = 2$, i.e., $2\times$ the transform limit. This value is significantly improved compared to previous measurements of quantum dots using above band gap excitation [39–44], including our own nanowire devices grown at a lower temperature [37]. It is also an improvement compared to measurements made using p -shell excitation

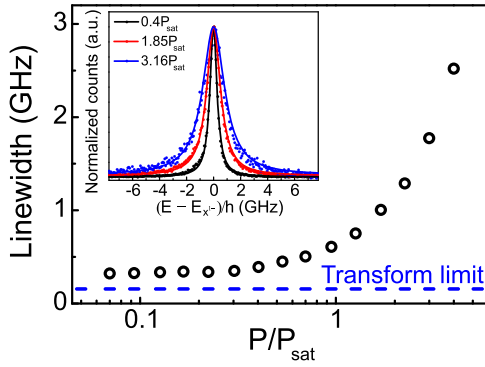


FIG. 2. Excitation power dependence of the homogeneous linewidth extracted from the PL spectra after deconvolution with the etalon response function. The inset shows the high-resolution PL spectra of the X^{1-} emission measured at $T = 4$ K for selected excitation powers. Solid lines correspond to Lorentzian fits to the data.

[40,44]. Instead, the values here are typically observed only when the emitter is excited resonantly [22,43,45,46] and are not significantly greater than those observed in state-of-the-art devices [8,44,47].

To verify if further reduction of the excess broadening is possible through improvement of the quality of the shell material, we have measured samples grown using higher shell growth temperatures. Increasing shell growth temperatures up to 495°C did not result in any further reductions of the linewidth, suggesting that the excess broadening is not related to defects in the shell material. Interestingly, we observed an increase in the axial growth rate with increasing temperature [see Fig. 1(a)] in contrast to previous experiments [38] where the axial growth was quenched at 450°C . This is likely due to a higher group V flux used for the shell growth in these experiments and raises the possibility of improving the material quality of the nanowire core by growing it at higher temperatures.

To rule out broadening associated with phonon dephasing, we performed both power- and temperature-dependent measurements. In Fig. 2 we show the linewidth dependence on excitation power for powers up to $P = 4P_{\text{sat}}$. All power-dependent spectra show Lorentzian line shapes (see inset) from which the homogeneous linewidths plotted in the figure are extracted. The dependence is highly nonlinear with the linewidth independent of excitation power for $P < 0.4P_{\text{sat}}$ above which strong broadening is observed.

In Fig. 3 we show temperature-dependent measurements under weak pumping conditions ($P < 0.2P_{\text{sat}}$). With increasing temperature the emission peak redshifts due to lattice dilation [48] and broadens. For temperatures up to $T = 14$ K the line shape remains Lorentzian while for $T > 14$ K a slight asymmetry develops. We focus on the spectra measured for $T \leq 14$ K from which we can extract the homogeneous linewidths plotted in the figure. Significant broadening is observed for $T > 8$ K while for $T < 8$ K, linewidths show only a small temperature dependence. We conclude that for sufficiently low temperatures ($T < 8$ K) and excitation powers ($P < 0.4P_{\text{sat}}$), phonon dephasing, notwithstanding above band gap excitation, is not the source of the remaining excess broadening. Instead, it likely arises from some residual

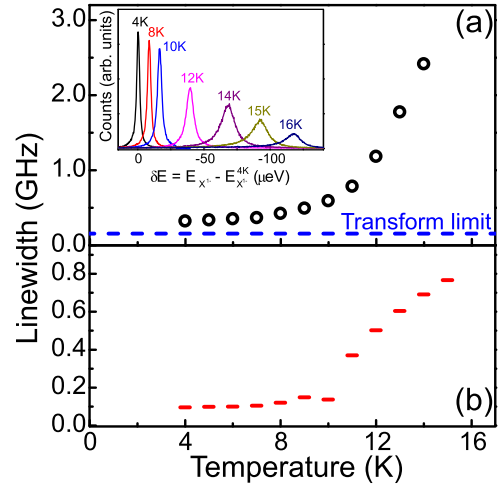


FIG. 3. (a) Deconvolved linewidth as a function of temperature in the low excitation power regime. The inset shows PL spectra, normalized to the integrated intensity, as a function of relative emission energy for selected temperatures. (b) Predicted broadening based on the model described in the text.

inhomogeneous broadening, that either does not sufficiently alter Lorentzian line shapes such that it can be revealed by a simple line-shape fitting procedure or that manifests as a homogeneous broadening [42].

III. THEORETICAL MODEL

We next consider the nonlinear behavior observed with temperature which is in stark contrast to the linear dependence seen in earlier studies [49] that also employed nonresonant excitation [39–41,50–52]. To date, the existence of the linear broadening is accounted for in InAs/GaAs zinc-blende dots by considering the independent boson model [34], in which the exciton causes a renormalization of phonon modes without itself being excited by the lattice vibrations. The origin of the quadratic term, on the other hand, is traced to the virtual transitions between the ground and excited exciton states caused by the absorption and reemission of the phonons [33,35]. In each of these approximations, only longitudinal phonon modes are accounted for, and the main exciton-phonon coupling mechanism is taken to be the deformation potential. In addition, the virtual transitions appear to be thermally activated only above a threshold temperature (of order of 10 K), below which only the linear broadening is expected [35]. Within this general approach, it is straightforward to understand the similarity between the linewidth broadening as a function of excitation power (Fig. 2) and as a function of temperature (Fig. 3). Indeed, above band gap excitation creates electron-hole pairs in the InP continuum with energy higher than the bare band gap. As the carriers have to thermalize before their capture by the quantum dot, phonons are necessarily generated, leading to an increase in the phonon mode population.

While we do not discount the possibility of a similar mechanism being present here, we do find that both the wurtzite lattice type of our system as well as its one-dimensional geometry suggest an alternative origin of

the nonlinear linewidth broadening. Indeed, the coupling between the carriers and the phonons is expressed as $M_a^{ij}(\vec{k}) = A_a(\vec{k}) \int d^3r \psi_{ia}^*(\vec{r}) \psi_{ja}(\vec{r}) e^{i\vec{k}\cdot\vec{r}}$, where the parameter $A_a(\vec{k})$ depends on the type of coupling (deformation or piezoelectric), material parameters, and phonon energy, \vec{k} is the phonon wave vector, and $\psi_{i,a}(\vec{r})$ is the wave function of the carrier a (electron or hole) corresponding to the single-particle state i [33–35]. Owing to the nanowire geometry, the only phonon modes with sufficiently low energy are those propagating along the wire, i.e., with $\vec{k} = [0, 0, k]$, while the lattice vibrations in the transverse direction are quantized with energies equivalent to hundreds of degrees Kelvin. As a result, the longitudinal phonon modes are unlikely to cause electronic transitions (even virtual ones) since they would need to straddle the intersubband energy gaps of hundreds of meV brought about by the small height of the quantum dot. This allows us to approximate, in the low phonon energy limit, $M_a^{ij}(\vec{k}) = A_a(\vec{k}) \delta_{i,j}$.

To date, the theoretical modeling of the linewidth broadening included the deformation potential as the only relevant mechanism of exciton-phonon coupling in zinc-blende materials [33–35] (see also Refs. [53,54] which include non-Markovian dephasing processes). Within the deformation-potential electron-phonon interaction, the coupling parameter for the one-dimensional phonon modes is $A_{\text{def}}(k) = \sqrt{\frac{\hbar\omega_k}{2\rho_M u_s^2 V}} D$, where the phonon energy $\hbar\omega_k = \hbar u_s k$, u_s is the speed of sound, ρ_M is the mass density, V is the phonon normalization volume, and $D = D_e - D_h$ is the deformation potential constant, expressed as the difference between the electron-phonon and hole-phonon coupling owing to the opposite signs of these charges. The piezoelectric coupling mechanism was found to be negligibly small, as it requires the shear strain tensor components, which are vanishingly small for longitudinal phonon modes. This is in contrast to the wurtzite crystal lattice, in which the piezoelectric effects enter through diagonal strain tensor element via the piezoelectric constant c_{33} . The relevant coupling parameter, adapted for the zinc-blende material from Ref. [34], has the form $A_{\text{piezo}}(k) = -16\pi e e_{33} \sqrt{\frac{\hbar^2}{2\rho_M \omega_k V}}$, where e is the electron charge. Crucially, the piezoelectric coupling has (i) the opposite sign to that of the deformation mechanism, and (ii) a different dependence on the phonon energy, $A_{\text{piezo}}(k) \propto (\omega_k)^{-1/2}$ compared to $A_{\text{def}}(k) \propto (\omega_k)^{1/2}$. As a result, the total coupling $A(k) = A_{\text{def}}(k) + A_{\text{piezo}}(k)$ is expected to depend strongly and nonlinearly on the phonon energy.

The X^{1-} emission spectra are calculated typically by considering the initial state composed of two electrons and a hole, and the final state composed of one electron, all interacting with phonons. In our simple model (see Supplemental Material [55]), we treat the extra electron as an inert spectator, as its contribution to particle-phonon interactions in the initial and final states is identical. This allows us to reduce the focus to the electron-hole pair. The Hamiltonian of the exciton-phonon system accounting for the approximations discussed above is

$$\hat{H}_{X-\text{ph}} = E_X |X\rangle\langle X| + \sum_{\vec{k}} \hbar\omega_{\vec{k}} a_{\vec{k}}^+ a_{\vec{k}} + \sum_{\vec{k}} A(|\vec{k}|) (a_{\vec{k}} + a_{\vec{k}}^+), \quad (1)$$

arising because the coupling $A(|\vec{k}|)$ depends only on the magnitude of the phonon wave vector $\vec{k} = [0, 0, k]$. Here, the operator $a_{\vec{k}}$ ($a_{\vec{k}}^+$) annihilates (creates) a phonon in mode \vec{k} . This independent boson model is exactly solvable in terms of displaced phonon operators $b_{\vec{k}} = a_{\vec{k}} + \Lambda_{\vec{k}}$ and $b_{\vec{k}}^+ = a_{\vec{k}}^+ + \Lambda_{\vec{k}}$, where the displacement $\Lambda_{\vec{k}} = A(k)/\hbar\omega_{\vec{k}}$. Upon this transformation, our Hamiltonian is diagonal both in the excitonic and phononic degrees of freedom and reads

$$\hat{H}_{X-\text{ph}} = E_X |X\rangle\langle X| + \sum_{\vec{k}} \hbar\omega_{\vec{k}} b_{\vec{k}}^+ b_{\vec{k}} - \sum_{\vec{k}} \hbar\omega_{\vec{k}} (\Lambda_{\vec{k}})^2. \quad (2)$$

The eigenvectors of our Hamiltonian can be written as the tensor products $|X\rangle \prod_{\vec{k}} |N_{\vec{k}}\rangle$, where the phonon Fock states $|N_{\vec{k}}\rangle = \frac{1}{\sqrt{N_{\vec{k}}!}} (b_{\vec{k}}^+)^{N_{\vec{k}}} |0\rangle$, and the state $|0\rangle$ is the zero-phonon state for the mode \vec{k} .

Upon exciton recombination, we deal with the system of nondisplaced phonons described simply by the Hamiltonian $\hat{H}_{\text{ph}} = \sum_{\vec{k}} \hbar\omega_{\vec{k}} a_{\vec{k}}^+ a_{\vec{k}}$ with eigenstates in the form of nondisplaced phonon Fock states $|n_{\vec{k}}\rangle = \frac{1}{\sqrt{n_{\vec{k}}!}} (a_{\vec{k}}^+)^{n_{\vec{k}}} |0\rangle$. Working with the Fock phonon configurations, both in the initial and final states of the system, and considering only one phonon mode with energy $\hbar\omega_{\vec{k}}$, we can now derive the emission spectrum in the form of a series of maxima found at energies

$$E(N_{\vec{k}}, n_{\vec{k}}, \Lambda_{\vec{k}}) = E_X - \hbar\omega_{\vec{k}} (\Lambda_{\vec{k}})^2 + \hbar\omega_{\vec{k}} (N_{\vec{k}} - n_{\vec{k}}). \quad (3)$$

The radiative transitions can be accompanied by phonon emission ($N_{\vec{k}} < n_{\vec{k}}$) or phonon absorption ($N_{\vec{k}} > n_{\vec{k}}$), placing the relevant maxima on the lower or higher side of the zero-phonon line, respectively. However, owing to the very small energy scale of the relevant phonon modes, the emission spectrum will be seen as a single, broadened peak, whose intensity will be modulated by an envelope expressed in terms of the well-known Franck-Condon formula

$$W(N_{\vec{k}}, n_{\vec{k}}, \Lambda_{\vec{k}}) = e^{-\Lambda_{\vec{k}}^2} \Lambda_{\vec{k}}^{2(n_{\vec{k}} - N_{\vec{k}})} \frac{N_{\vec{k}}!}{n_{\vec{k}}!} \left[L_{N_{\vec{k}} - n_{\vec{k}}}^{n_{\vec{k}} - N_{\vec{k}}} (\Lambda_{\vec{k}}^2) \right]^2, \quad (4)$$

where $n_{\vec{k}} \geq N_{\vec{k}}$ and $L_n^m(x)$ is the associated Laguerre polynomial (for $n_{\vec{k}} < N_{\vec{k}}$ the indices are interchanged).

The emission spectrum as a function of temperature T and accounting for statistical occupation of the phonon modes is computed as a weighted superposition of the single-mode spectra. Upon normalization by the zero-phonon line intensity, we have

$$I(\hbar\omega, T) \propto \sum_{\vec{k}} \frac{1}{I_0(\vec{k})} \sum_{N_{\vec{k}}} \sum_{n_{\vec{k}}} p(N_{\vec{k}}, T) W(N_{\vec{k}}, n_{\vec{k}}, \Lambda_{\vec{k}}) \times \delta(\hbar\omega - E(N_{\vec{k}}, n_{\vec{k}}, \Lambda_{\vec{k}})), \quad (5)$$

with $\hbar\omega$ being the measured photon energy. Here, we consider all possible initial and final occupations of each phonon mode \vec{k} , weighted by the probabilities $p(N_{\vec{k}}, T) = \exp(-\frac{N_{\vec{k}} \hbar\omega_{\vec{k}}}{k_B T}) / Z(\vec{k})$, where the statistical sum $Z(\vec{k}) = \sum_{n=0}^{\infty} \exp(-\frac{n \hbar\omega_{\vec{k}}}{k_B T})$, and k_B is the Boltzmann constant. The modal zero-phonon line intensity is $I_0(\vec{k}) = \sum_{N_{\vec{k}}} p(N_{\vec{k}}, T) |\langle n_{\vec{k}} = N_{\vec{k}} | N_{\vec{k}} \rangle|^2$. Our approach takes into account the fact that, calculated individually, the low

occupations of any given phonon mode \vec{k} are exponentially more probable than the high occupations, and therefore give more contribution to the overall emission spectrum.

We propose that the experimentally observed nonlinearity of the emission peak broadening is captured by our model, even without the virtual excitation scheme, in two aspects. The first crucial aspect is the dependence of the displacement parameter $\Lambda_{\vec{k}}$ on the phonon mode energy $\hbar\omega_{\vec{k}}$. We have $\Lambda_{\vec{k}} = \Lambda_{\vec{k}}^{(\text{def})} - \Lambda_{\vec{k}}^{(\text{piezo})} = \Lambda_0^{(\text{def})}(\hbar\omega_{\vec{k}})^{-1/2} - \Lambda_0^{(\text{piezo})}(\hbar\omega_{\vec{k}})^{-3/2}$, where $\Lambda_0^{(\text{def})}$ and $\Lambda_0^{(\text{piezo})}$ are energy-independent material constants describing the two coupling mechanisms, respectively. Even if the piezoelectric coupling constant is smaller than the deformation one, at sufficiently small phonon energies these two terms will cancel each other out, giving the overall displacement parameter of zero. As the material parameters for wurtzite InAs and InP are not yet known, our experimental data suggest that this cancellation occurs most likely for phonon energies of order of 0.1 μeV , resulting in the very small emission peak broadening for low temperatures. On the other hand, at higher phonon energies the piezoelectric contribution to the parameter $\Lambda_{\vec{k}}$ decays faster than the deformation one, resulting in an effective, nonlinear increase of that parameter. As a result, the higher-energy modes, which become more populated at higher temperatures, cause the peak broadening visible at higher temperatures.

The crossover between the two regimes is systematically accounted for by the second aspect of our model, i.e., the mode occupation probabilities $p(N_{\vec{k}}, T)$. As already mentioned, at low temperatures these probabilities strongly favor low-energy modes occupied with few phonons, for which the effective exciton-phonon coupling is negligibly small due to the cancellation discussed above. However, as the temperature increases, the probabilities are redistributed towards increasing occupations of more energetic phonon modes, which are more strongly coupled to the exciton. As a result, these higher modes contribute more to the emission spectrum, resulting in the nonlinear increase of the peak broadening.

We illustrate the above theoretical model with a calculation accounting for four phonon modes, with energies $\hbar\omega_{\vec{k}} =$

0.25, 0.5, 1, and 2 μeV . We chose the following dependence of the displacement parameter on the mode energy, $\Lambda(\varepsilon) = A_0(\varepsilon^{-1/2} - \varepsilon^{-3/2})$, where $\varepsilon = \hbar\omega_{\vec{k}}/\varepsilon_0$, $\varepsilon_0 = 0.1 \mu\text{eV}$, and A_0 was taken as a model value of 0.2. This functional form follows directly from the subtraction of the deformation and piezoelectric contributions, and was adjusted to vanish for $\hbar\omega_{\vec{k}} = 0.1 \mu\text{eV}$. We generated the emission spectra at a grid of photon energies with steps of 2 μeV on both sides of the zero-phonon line, but we excluded the zero-phonon line itself, as its emission peak contains contributions from all phonon modes present in the system and therefore would be poorly reproduced by our model. The full width at half maximum (FWHM) obtained by fitting the resulting emission peak by a Lorentzian is presented in Fig. 3. Unsurprisingly, the theoretical approach, accounting only for four modes, underestimates the line broadening, but reproduces the experimental temperature trend qualitatively.

In summary, we have shown that it is possible to generate near-transform-limited photons from quantum dots, even when excited above the band gap, by using structures that eliminate many potential broadening mechanisms. The drastic reduction in excess broadening revealed a nonlinear temperature dependence that can be fully described within an independent boson model that considers both deformation and piezoelectric coupling mechanisms, the latter expected to be more important in these wurtzite structures compared to the more typical zinc-blende quantum dots.

The data that support the findings of this study are available from the corresponding author upon reasonable request.

ACKNOWLEDGMENTS

This work was supported by the Natural Sciences and Engineering Research Council of Canada through the Discovery Grant SNQLS, by the National Research Council of Canada through the Small Teams Ideation Program QPIC, and by the Canadian Space Agency through a collaborative project entitled “Field Deployable Single Photon Emitters for Quantum Secured Communications.”

- [1] J. L. O’Brien, A. Furusawa, and J. Vučković, Photonic quantum technologies, *Nat. Photonics* **3**, 687 (2009).
- [2] I. Aharonovich, D. Englund, and M. Toth, Solid-state single-photon emitters, *Nat. Photonics* **10**, 631 (2016).
- [3] P. Senellart, G. Solomon, and A. White, High-performance semiconductor quantum-dot single-photon sources, *Nat. Nanotechnol.* **12**, 1026 (2017).
- [4] H. Vural, S. L. Portalupi, and P. Michler, Perspective of self-assembled InGaAs quantum-dots for multi-source quantum implementations, *Appl. Phys. Lett.* **117**, 030501 (2020).
- [5] J.-M. Gérard and B. Gayral, Strong Purcell effect for InAs quantum boxes in three-dimensional solid-state microcavities, *J. Lightwave Technol.* **17**, 2089 (1999).
- [6] X. Ding, Y. He, Z.-C. Duan, N. Gregersen, M.-C. Chen, S. Unsleber, S. Maier, C. Schneider, M. Kamp, S. Höfling, C.-Y. Lu, and J.-W. Pan, On-Demand Single Photons with High

- Extraction Efficiency and Near-Unity Indistinguishability from a Resonantly Driven Quantum Dot in a Micropillar, *Phys. Rev. Lett.* **116**, 020401 (2016).
- [7] A. Müller, E. B. Flagg, P. Bianucci, X.Y. Wang, D. G. Deppe, W. Ma, J. Zhang, G. J. Salamo, M. Xiao, and C. K. Shih, Resonance Fluorescence from a Coherently Driven Semiconductor Quantum Dot in a Cavity, *Phys. Rev. Lett.* **99**, 187402 (2007).
- [8] H. Wang, Z.-C. Duan, Y.-H. Li, Si Chen, J.-P. Li, Y.-M. He, M.-C. Chen, Y. He, X. Ding, C.-Z. Peng, C. Schneider, M. Kamp, S. Höfling, C.-Y. Lu, and J.-W. Pan, Near-Transform-Limited Single Photons from an Efficient Solid-State Quantum Emitter, *Phys. Rev. Lett.* **116**, 213601 (2016).
- [9] N. Tomm, A. Javadi, N. O. Antoniadis, D. Najer, M. C. Löbl, Al. R. Korsch, R. Schott, S. R. Valentin, A. D. Wieck, A. Ludwig, and R. J. Warburton, A bright and fast source of coherent single photons, *Nat. Nanotechnol.* **16**, 399 (2021).

- [10] We note that since pulsed excitation, required for on-demand operation, is spectrally broader compared to cw excitation, it is less effective in mitigating linewidth broadening,
- [11] R. B. Patel, A. J. Bennett, I. Farrer, C. A. Nicoll, D. A. Ritchie, and A. J. Shields, Two-photon interference of the emission from electrically tunable remote quantum dots, *Nat. Photonics* **4**, 632 (2010).
- [12] E. B. Flagg, A. Muller, S. V. Polyakov, A. Ling, A. Migdall, and Glenn S. Solomon, Interference of Single Photons from Two Separate Semiconductor Quantum Dots, *Phys. Rev. Lett.* **104**, 137401 (2010).
- [13] W. B. Gao, P. Fallahi, E. Togan, A. Delteil, Y. S. Chin, J. Miguel-Sanchez, and A. Imamoglu, Quantum teleportation from a propagating photon to a solid-state spin qubit, *Nat. Commun.* **4**, 2744 (2016).
- [14] P. Gold, A. Thoma, S. Maier, S. Reitzenstein, C. Schneider, S. Höfling, and M. Kamp, Two-photon interference from remote quantum dots with inhomogeneously broadened linewidths, *Phys. Rev. B* **89**, 035313 (2014).
- [15] V. Giesz, S. L. Portalupi, T. Grange, C. Antón, L. De Santis, J. Demory, N. Somaschi, I. Sagnes, A. Lemaître, L. Lanco, A. Auffeves, and P. Senellart, Cavity-enhanced two-photon interference using remote quantum dot sources, *Phys. Rev. B* **92**, 161302(R) (2015).
- [16] M. Reindl, K. D. Jöns, D. Huber, C. Schimpf, Y. Huo, V. Zwiller, A. Rastelli, and R. Trotta, Phonon-assisted two-photon interference from remote quantum emitters, *Nano Lett.* **17**, 4090 (2017).
- [17] J. H. Weber, J. Kettler, H. Vural, M. Müller, J. Maisch, M. Jetter, S. L. Portalupi, and P. Michler, Overcoming correlation fluctuations in two-photon interference experiments with differently bright and independently blinking remote quantum emitters, *Phys. Rev. B* **97**, 195414 (2018).
- [18] H. D. Robinson and B. B. Goldberg, Light-induced spectral diffusion in single self-assembled quantum dots, *Phys. Rev. B* **61**, R5086 (2000).
- [19] B. D. Gerardot, R. J. Barbour, D. Brunner, A. Badolato P. A. Dalgarno and, N. Stoltz, P. M. Petroff, J. Houel, and R. J. Warburton, Laser spectroscopy of individual quantum dots charged with a single hole, *Appl. Phys. Lett.* **99**, 243112 (2011).
- [20] C. F. Wang, A. Badolato, P. M. Petroff I. Wilson-Rae and, and E. Hu, Optical properties of single InAs quantum dots in close proximity to surfaces, *Appl. Phys. Lett.* **85**, 3423 (2004).
- [21] J. Liu, K. Konthasinghe, M. Davanço, J. Lawall, V. Anant, V. Verma, R. Mirin, S. W. Nam, J. D. Song, B. Ma, Z. S. Chen, H. Q. Ni, Z. C. Niu, and K. Srinivasan, Single Self-Assembled InAs/GaAs Quantum Dots in Photonic Nanostructures: The Role of Nanofabrication, *Phys. Rev. Appl.* **9**, 064019 (2018).
- [22] J. Houel, A. V. Kuhlmann, L. Greuter, F. Xue, M. Poggio, B. D. Gerardot, P. A. Dalgarno, A. Badolato, P. M. Petroff, A. Ludwig, D. Reuter, A. D. Wieck, and R. J. Warburton, Probing Single-Charge Fluctuations at a GaAs/AlAs Interface using Laser Spectroscopy on a Nearby InGaAs Quantum Dot, *Phys. Rev. Lett.* **108**, 107401 (2012).
- [23] M. B. Bavinck, K. D. Jöns, M. Zieliński, G. Patriarache, J.-C. Harmand, N. Akopian, and V. Zwiller, Photon cascade from a single crystal phase nanowire quantum dot, *Nano Lett.* **16**, 1081 (2016).
- [24] D. Dalacu, P. J. Poole, and R. L. Williams, Nanowire-based sources of non-classical light, *Nanotechnology* **30**, 232001 (2019).
- [25] P. Laferrière, E. Yeung, I. Miron, D. B. Northeast, S. Haffouz, J. Lapointe, M. Korkusinski, P. J. Poole, R. L. Williams, and D. Dalacu, Unity yield of deterministically positioned quantum dot single photon sources, *Sci. Rep.* **12**, 6376 (2022).
- [26] C. P. Dietrich, A. Fiore, M. G. Thompson, M. Kamp, and S. Höfling, Gaas integrated quantum photonics: Towards compact and multi-functional quantum photonic integrated circuits, *Laser Photonics Rev.* **10**, 870 (2016).
- [27] J. Claudon, J. Bleuse, N. S. Malik, M. Bazin, P. Jaffrennou, N. Gregersen, C. Sauvan, P. Lalanne, and J.-M. Gérard, A highly efficient single-photon source based on a quantum dot in a photonic nanowire, *Nat. Photonics* **4**, 174 (2010).
- [28] C. A. Hoffman, H. J. Gerritsen, and A. V. Nurmikko, Study of surface recombination in GaAs and InP by picosecond optical techniques, *J. Appl. Phys.* **51**, 1603 (1980).
- [29] M. Borgström, V. Zwiller, E. Müller, and A. Imamoglu, Optically bright quantum dots in single nanowires, *Nano Lett.* **5**, 1439 (2005).
- [30] M. C. Löbl, S. Scholz, I. Söllner, J. Ritzmann, T. Denneulin, A. Kovács, B. E. Kardynał, A. D. Wieck, A. Ludwig, and R. J. Warburton, Excitons in InGaAs quantum dots without electron wetting layer states, *Commun. Phys.* **2**, 93 (2018).
- [31] P. Laferrière, E. Yeung, L. Giner, S. Haffouz, J. Lapointe, G. C. Aers, P. J. Poole, R. L. Williams, and D. Dalacu, Multiplexed single-photon source based on multiple quantum dots embedded within a single nanowire, *Nano Lett.* **20**, 3688 (2020).
- [32] P. Borri, W. Langbein, U. Woggon, V. Stavarache, D. Reuter, and A. D. Wieck, Exciton dephasing via phonon interactions in InAs quantum dots: Dependence on quantum confinement, *Phys. Rev. B* **71**, 115328 (2005).
- [33] A. Reigue, J. Iles-Smith, F. Lux, L. Monniello, M. Bernard, F. Margaillan, A. Lemaître, A. Martinez, D. P. S. McCutcheon, J. Mørk, R. Hostein, and V. Voliotis, Probing Electron-Phonon Interaction through Two-Photon Interference in Resonantly Driven Semiconductor Quantum Dots, *Phys. Rev. Lett.* **118**, 233602 (2017).
- [34] T. Takagahara, Theory of exciton dephasing in semiconductor quantum dots, *Phys. Rev. B* **60**, 2638 (1999).
- [35] E. A. Muljarov and R. Zimmermann, Dephasing in Quantum Dots: Quadratic Coupling to Acoustic Phonons, *Phys. Rev. Lett.* **93**, 237401 (2004).
- [36] D. Dalacu, K. Mnaymneh, X. Wu, J. Lapointe, G. C. Aers, P. J. Poole, and R. L. Williams, Selective-area vapor-liquid-solid growth of tunable InAsP quantum dots in nanowires, *Appl. Phys. Lett.* **98**, 251101 (2011).
- [37] M. E. Reimer, G. Bulgarini, A. Fognini, R. W. Heeres, B. J. Witek, M. A. M. Versteegh, A. Rubino, T. Braun, M. Kamp, S. Höfling, D. Dalacu, J. Lapointe, P. J. Poole, and V. Zwiller, Overcoming power broadening of the quantum dot emission in a pure wurtzite nanowire, *Phys. Rev. B* **93**, 195316 (2016).
- [38] D. Dalacu, A. Kam, D. G. Austing, X. Wu, J. Lapointe, G. C. Aers, and P. J. Poole, Selective-area vapour-liquid-solid growth of InP nanowires, *Nanotechnology* **20**, 395602 (2009).
- [39] D. Birkedal, K. Leosson, and J. M. Hvam, Long Lived Coherence in Self-Assembled Quantum Dots, *Phys. Rev. Lett.* **87**, 227401 (2001).

- [40] M. Bayer and A. Forchel, Temperature dependence of the exciton homogeneous linewidth in $\text{In}_{0.60}\text{Ga}_{0.40}\text{As}/\text{GaAs}$ self-assembled quantum dots, *Phys. Rev. B* **65**, 041308(R) (2002).
- [41] B. Urbaszek, E. J. McGhee, M. Krüger, R. J. Warburton, K. Karrai, T. Amand, B. D. Gerardot, P. M. Petroff, and J. M. Garcia, Temperature-dependent linewidth of charged excitons in semiconductor quantum dots: Strongly broadened ground state transitions due to acoustic phonon scattering, *Phys. Rev. B* **69**, 035304 (2004).
- [42] A. Berthelot, I. Favero, G. Cassaboïs, C. Voisin, C. Delalande, Ph. Roussignol, R. Ferreira, and J. M. Gérard, Unconventional motional narrowing in the optical spectrum of a semiconductor quantum dot, *Nat. Phys.* **2**, 759 (2006).
- [43] A. V. Kuhlmann, J. Houel, A. Ludwig, L. Greuter, D. Reuter, A. D. Wieck, M. Poggio, and R. J. Warburton, Charge noise and spin noise in a semiconductor quantum device, *Nat. Phys.* **9**, 570 (2013).
- [44] Y.-M. He, Y. He, Y.-J. Wei, D. Wu, M. Atatüre, C. Schneider, S. Höfling, M. Kamp, C.-Y. Lu, and J.-W. Pan, On-demand semiconductor single-photon source with near-unity indistinguishability, *Nat. Nanotechnol.* **8**, 213 (2013).
- [45] A. Högele, S. Seidl, M. Kroner, K. Karrai, R. J. Warburton, B. D. Gerardot, and P. M. Petroff, Voltage-Controlled Optics of a Quantum Dot, *Phys. Rev. Lett.* **93**, 217401 (2004).
- [46] M. Atatüre, J. Dreiser, A. Badolato, A. Högele, K. Karrai, and A. Imamoglu, Quantum-dot spin-state preparation with near-unity fidelity, *Science* **312**, 551 (2006).
- [47] A. V. Kuhlmann, J. H. Prechtel, J. Houel, A. Ludwig, D. Reuter, A. D. Wieck, and R. J. Warburton, Transform-limited single photons from a single quantum dot, *Nat. Commun.* **6**, 8204 (2015).
- [48] Y.P. Varshni, Temperature dependence of the energy gap in semiconductors, *Physica* **34**, 149 (1967).
- [49] We note that in these studies the excess broadening was significantly greater than that presented here and has been described in terms of phonon scattering from sidewalls and interfaces [56].
- [50] L. Besombes, K. Kheng, L. Marsal, and H. Mariette, Acoustic phonon broadening mechanism in single quantum dot emission, *Phys. Rev. B* **63**, 155307 (2001).
- [51] G. Ortner, D. R. Yakovlev, M. Bayer, S. Rudin, T. L. Reinecke, S. Fafard, Z. Wasilewski, and A. Forchel, Temperature dependence of the zero-phonon linewidth in $\text{In}(\text{Ga})\text{As}/(\text{Al})\text{GaAs}$ quantum dots, *Phys. Rev. B* **70**, 201301(R) (2004).
- [52] I. Favero, A. Berthelot, G. Cassaboïs, C. Voisin, C. Delalande, Ph. Roussignol, R. Ferreira, and J.-M. Gérard, Temperature dependence of the zero-phonon linewidth in quantum dots: An effect of the fluctuating environment, *Phys. Rev. B* **75**, 073308 (2007).
- [53] H. Tahara, Y. Ogawa, and F. Minami, Non-Markovian Dynamics of Spectral Narrowing for Excitons in the Layered Semiconductor GaSe Observed Using Optical Four-Wave Mixing Spectroscopy, *Phys. Rev. Lett.* **107**, 037402 (2011).
- [54] H. Tahara, Y. Ogawa, F. Minami, K. Akahane, and M. Sasaki, Long-Time Correlation in Non-Markovian Dephasing of an Exciton-Phonon System in InAs Quantum Dots, *Phys. Rev. Lett.* **112**, 147404 (2014).
- [55] See Supplemental Material at <http://link.aps.org/supplemental/10.1103/PhysRevB.107.155422> for details of the model used to calculate Fig. 3(b), which includes Ref. [57].
- [56] S. Rudin, T. L. Reinecke, and M. Bayer, Temperature dependence of optical linewidth in single InAs quantum dots, *Phys. Rev. B* **74**, 161305(R) (2006).
- [57] M. Cygorek, M. Korkusinski, and P. Hawrylak, Atomistic theory of electronic and optical properties of InAsP/InP nanowire quantum dots, *Phys. Rev. B* **101**, 075307 (2020).